Chandra Observations of Point Sources in Abell 2255

David S. Davis[1,2]

Neal A. Miller[3]

and

Richard F. Mushotzky[4]

ABSTRACT

In our search for "hidden" AGN we present results from a *Chandra* observation of the nearby cluster Abell 2255. Eight cluster galaxies are associated with point-like X-ray emission, and we classify these galaxies based on their X-ray, radio, and optical properties. At least three are associated with active galactic nuclei (AGN) with no optical signatures of nuclear activity, with a further two being potential AGN. Of the potential AGN, one corresponds to a galaxy with a post-starburst optical spectrum. The remaining three X-ray detected cluster galaxies consist of two starbursts and an elliptical with luminous hot gas. Of the eight cluster galaxies five are associated with luminous (massive) galaxies and the remaining three lie in much lower luminosity systems. We note that the use of X-ray to optical flux ratios for classification of X-ray sources is often misleading, and strengthen the claim that the fraction of cluster galaxies hosting an AGN based on optical data is signficantly lower than the fraction based on X-ray and radio data.

Subject headings: galaxies: clusters: individual (Abell 2255) — galaxies: clusters: general — galaxies: active — galaxies: intergalactic medium — X-rays: galaxies

[1]Laboratory for High Energy Astrophysics, Code 661, Greenbelt, MD 20771

[2]Joint Center for Astrophysics, Department of Physics, University of Maryland, Baltimore County, 1000 Hilltop Circle, Baltimore, MD 21250

[3]NASA/GSFC UV/Optical Branch, Code 681, Greenbelt, MD 20771

[4]Laboratory for High Energy Astrophysics, Code 662, Greenbelt, MD 20771

1.   Introduction

Until fairly recently it has been thought that, at least at low redshift, the relative fraction of active galaxies in rich clusters was considerably lower than in the field (Dressler & Gunn 1983; Yee & Ellingson 1993; Dressler et al. 1999). Recent *Chandra* observations have revealed a more substantial population of active galactic nuclei (AGN) in clusters of galaxies (Cappi et al. 2001; Sun & Murray 2002; Molnar et al. 2002; Martini et al. 2002). Optically, the hosts of these sources often appear relatively unremarkable: they have colors consistent with cluster ellipticals, and optical spectra lacking emission lines. Thus, traditional optical studies overlook these sources and arrive at a fraction of $\sim 1\%$ of all cluster galaxies harboring an AGN (e.g., Dressler et al. 1999). Including these X-ray selected AGN, however, yields a fraction of $\sim 5\%$, consistent with the fraction of field galaxies hosting an AGN on the basis of optical studies (Barger et al. 2002).

Interestingly enough, similar results have been found via radio continuum studies. The classical radio galaxies, with large jets and lobes of radio emission, are one such example. Yet these sources are rare, and typical clusters of galaxies only contain up to a few such radio galaxies (Ledlow & Owen 1995). However, more sensitive observations have continued to reveal fainter compact radio sources in elliptical galaxies, most of which are thought to be AGN (e.g., Sadler, Jenkins, & Kotanyi 1989), and most of which have optical spectra exhibiting no emission lines or weak [NII] emission (Phillips et al. 1986). The incidence of such AGN in clusters of galaxies appears to be consistent with that inferred from the recent X-ray studies (Miller & Owen 2002).

The importance of these AGN is potentially significant. Martini et al. (2002) note that a large population of cluster AGN would do much to explain the hard X-ray background. Variations in the X-ray background across the sky (e.g., Cowie et al. 2002) would be a natural consequence of cosmological structure and the cluster distribution. Furthermore, studies based on optical properties of galaxies are clearly overlooking a large number of active galaxies. This complicates analyses of evolutionary trends. Evidence for this is seen in recent X-ray surveys (Barger et al. 2002; Hasinger 2003) which show that X-ray selected objects evolve rather differently from optically selected ones and that the space density of X-ray selected AGN is considerably larger than that of optically selected objects.

Clusters of galaxies are attractive for studying galaxy evolution because they contain large numbers of galaxies all at the same redshift. Thus, samples of AGN derived from a given cluster are subject to the same selection effects. Comparisons among the cluster-selected AGN may thereby be used to investigate questions such as the nature of the X-ray selected, optically "dull" galaxies (Elvis et al. 1980). In addition, we seek to address if and why the fraction of optically-selected AGN in clusters differs from that in the field. As data

for more clusters becomes available, the question of why the environment of optically-selected objects changes rapidly with redshift (Yee & Ellingson 1993) may be addressed.

The question of how the cluster enviroment affects the nuclear activity is also an interesting question. Nuclear activity in galaxies is thought to be powered by accretion onto a supermassive black hole. Over the long term this accretion must be fueled by gas on the galactic scale transported into the inner few kpc of the galaxy. This transport can be triggered by mergers and interactions of galaxies (e.g., Hernquist 1989). The interactions of major clusters may also increase the activity of member galaxies (Metevier et al. 2000).

Abell 2255 is a rich cluster which shows several signs that it is undergoing a merger event. Some of the first evidence for a merger came from early *Einstein* X-ray data: Jones & Forman (1984) found that Abell 2255 has one of the largest X-ray core radii in their cluster sample. Stewart et al. (1984) further analyzed *Einstein* IPC data and concluded that Abell 2255 does not contain a cooling flow, which is unusual for such a rich cluster (Edge, Stewart, & Fabian 1992). Under certain conditions, major mergers may disrupt pre-existing cooling flows and increase the core radius of X-ray gas (Gómez et al. 2002). More recently, analyses of *ROSAT* data have confirmed the X-ray elongation and noted that the X-ray peak of Abell 2255 is not centered on the brightest cluster galaxies but is offset by $\sim 2'$ (Burns et al. 1995; Feretti et al. 1997). Thus, the X-ray data indicate that this cluster has recently undergone or is currently undergoing a merger. Optically, Abell 2255 has a very large velocity dispersion, ≈ 1200 km s^{-1}, and shows evidence for kinematical substructure in the form of several associated groups (Hill et al. 2003). The large ratio of velocity dispersion to X-ray temperature (6.3 keV, Horner 2001) also indicates a non-relaxed system. Furthermore, Abell 2255 contains two comparably bright central dominant galaxies, which is reminiscent of the Coma cluster and indicative of a merger of separate clusters (Davis & Mushotzky 1993; Bird 1994). Abell 2255 is also one of the rare clusters which contains a radio halo (Jaffe & Rudnick 1979; Hanisch 1982; Feretti et al. 1997). To date, radio halos have only been detected in clusters which exhibit signatures of mergers.

Here we present *Chandra* data for the relatively nearby cluster Abell 2255 ($z = 0.08$) showing that eight of the galaxies in the central region of the cluster are unresolved or small X-ray sources. This cluster represents an excellent opportunity to revisit the question of X-ray selected AGN in clusters, as a deep radio continuum survey of the cluster has recently been performed (Miller & Owen 2003) and high quality optical spectra are available through the Sloan Digital Sky Survey Early Data Release (SDSS, Stoughton et al. 2002). Thus, the active galaxies in an X-ray selected sample may be evaluated over a broad wavelength range in order to better assess the origin of the activity and how it might be surmised.

2. Data and Analysis

2.1. X-Ray

Abell 2255 was observed with the ACIS-I detector (Garmire et al. 2003) on the *Chandra* observatory for a total of 39 ksec on October 20 - 21 2000. Examining the lightcurve from chip 7 (the back illuminated CCD) we excluded a small background enhancement at the beginning of the exposure. This left a total of ∼34.7 ksec of exposure time.

X-ray images of the Abell 2255 field are shown in Figures 1 and 2. In the first figure, the data have been smoothed with a Gausssian with a σ of $1''$ to emphasize the point sources, which may be seen along with the diffuse X-ray emission from the cluster. The second figure depicts the X-ray emission along with the radio contours (Miller & Owen 2003, see Section 2.2). We used the CIAO program WAVDETECT to detect X-ray point sources in the field and visually confirmed the detections. We used a sensitivity threshold of 10^{-6}, which gives about 1 false detection per 1024x1024 ACIS chip if background is spatially uniform (Freeman et al. 2002). These sources were checked against the SDSS data and the velocity data from Hill et al. (2003) for the region. Only sources that lay in the velocity range of 20,289 – 27,705 km s^{-1} were identified as cluster sources (i.e., sources within $\pm 3\sigma$ of the cluster systemic velocity, using the biweight estimators of Beers, Flynn, & Gebhardt 1990). This resulted in a list of eight galaxies in the cluster center, which are listed in Table 1 and henceforth referred to by the ID numbers designated in that table. The columns in table 1 are the ID, the source name, the power law index, the X-ray luminosity in the $0.5 – 10$ keV band (assuming $H_0 = 50$ km/s/Mpc, $q_0=0$.), the 20cm radio flux, the r* magnitudes and g$^*-$r* colors are determined from the SDSS data. The radial velocities we used are in the final column.

We used *XSPEC 11.2.o* software (Arnaud 1996) to fit a spectral model to the extracted spectra. We extracted the spectra using an aperture with a radius of $10''$ for the point sources and $20''$ for the extended source to obtain all the flux. The background for each spectrum was obtained from a ring from outside the source region. This removes the underlying cluster emission as well as the normal background components. Finally, the extracted spectra were rebinned so that each channel had a minimum of 25 counts.

For the brightest source (#1 in Table 1) we fit the spectrum with a power law plus a contribution from a soft thermal component associated with the galaxy. All fits included a component for the extra absoption on the ACIS detectors (acisabs in XSPEC) and a variable absorption component due to the column density of Galactic hydrogen in the line-of-sight. The redshift of the model spectrum was fixed to the heliocentric velocity of the cluster. For the other sources with sufficient counts we fit a simple power law model, or if there were

too few counts for spectral fitting we estimated the flux by fixing the index of the power law model to 1.7. The extracted spectra were fit between ∼0.5 and 9.0 keV, with the exact energy boundaries being set by the channel grouping. Once a minimum in χ^2 was found, the 90% confidence errors were determined for the free parameters. For the weaker sources, hardness ratios were calculated in the 0.5–1.5, 1.5–2.5, and 2.5–4.0 keV bands and compared to simple thermal and power law models.

The X-ray spectrum for source #1 is shown in Figure 3. The model fit here is an APEC model for the thermal plasma and a power law model. The thermal component has a temperature of $0.15^{+0.05}_{-0.11}$ keV with a best fit abundance of zero, but the upper limit on the abundance is unconstrained. The power law spectrum has a photon index of $2.98^{+0.86}_{-1.08}$. For this fit the absorption is fixed to the Galactic value and the resulting χ^2 is 8.8 for 9 degrees of freedom. A pure power law or thermal plasma model is a poor fit to the spectrum with a reduced χ^2 of 1.53 for 11 degrees of freedom. The unabsorbed luminosity in the 0.5-10 keV band is 2.0×10^{42} ergs s^{-1}. The 2-10 keV luminosity of 3.7×10^{41} ergs s^{-1} is typical of weak-line radio galaxies (Sambruna, Eracleous & Mushotzky 1999) although the oxygen lines usually seen in these objects are not present in the SDSS spectrum (see Figure 4 and Section 2.3). The large fitted photon index has been seen in other objects such as NGC 3862 (Sun & Murray 2002) and in BL Lac objects (Ciliegi, Bassani, & Caroli 1995; Kubo et al. 1998). The KPNO image is shown in Figure 5 with the X-ray contours from the smoothed *Chandra* image overlaying the optical.

Sources #2, #3, #7 & #8 have too few counts for a spectral fit so their luminosities are estimated using a power law with the index fixed to 1.7. We fit the stacked spectra of these sources to test our assumption that this power law was appropriate and found that combined spectral fit was consistent with an index of 1.7. The optical images are shown in Figures 5b, 5c, 5g and 5h. In figure 5h the X-ray peak is offset from the optical center of the galaxy by 3″.3. We have checked the astrometry by measuring the position of a known star (N1121133294 from the GSC 2.1) and find it offset from the X-ray position by ∼1″.1. The average offset between the point-like X-ray and radio sources is 1″.5. Given the larger than average offset source # 8 may be an ultraluminous X-ray source (Makishima et al. 2000). However, given the lack of other astrometric references we cannot be certain of this.

The morphology of Source #4 is more complex and shows signs of possible extent (Figure 5d). The 50% encircled energy radius for this source is 3″.1, larger than the predicted value of ∼2″ at this off-axis angle, and consistent with this being extended thermal emission from an elliptical galaxy. In addition, the spectrum is better fit with a thermal plasma than with a power law. The fitted *APEC* model yields a temperature of $0.57^{+0.49}_{-0.32}$ keV and an abundance less than 0.63 solar which is typical for elliptical galaxies (Davis & White 1996).

Source #5 is fit with fairly large power law index and there is marginal evidence in the X-ray spectrum for a soft component like that seen in source #1. However, the net counts for this source are such that the inclusion of a soft thermal component is not statistically required and the X-ray contours in Figure 5e do not show any evidence for extended emission.

Source #6 has sufficent counts for a fit and the resulting power law is typical of active galaxies with a photon index of $1.75^{+1.90}_{-0.78}$. The X-ray contours in Figure 5f show a strong point source associated with the nucleus of the galaxy.

2.2.   Radio

Radio continuum imaging of Abell 2255 was performed using the National Radio Astronomy Observatory's Very Large Array (VLA).[5] The observations and reductions are described in Miller & Owen (2003). Briefly, the cluster was surveyed at a frequency of 1.4GHz (20cm) using a 25-pointing mosaic. Each pointing had a duration of $\sim$ 25 minutes total, and the final map had an rms noise of $\sim 40\mu$Jy beam^{-1} for a 5.9″ beam. Adopting a 5σ detection limit, over 50 cluster radio galaxies were identified out to fairly large radii ($\sim 40'$) from the cluster center.

Abell 2255 has an unusually high number of radio galaxies relative to other nearby Abell clusters (Miller & Owen 2003). These fall into two generalized categories: bright elliptical galaxies hosting AGN and faint spiral and irregular starbursts. The AGN are often spectacular radio sources, including six sources with extended radio emission. Four of these lie within the field surveyed by our *Chandra* observations and may be seen in Figure 2. Three of these are "head-tail" radio sources in which the host galaxy lies at one end of the radio emission which extends in a "tail" well past the edge of the galaxy, while the fourth is a strong compact double.

The correspondence of the radio sources and the *Chandra* sources is excellent. There are 16 cluster radio galaxies in the general region covered by the *Chandra* observations, including all eight of the detections. Only three of the four extended radio galaxies are associated with *Chandra* detections; but on closer inspection, the non-detection of the fourth (J171223+640157) is easily explained as by chance it lies between the CCDs of the ACIS-I detector. Hence, eight of 15 cluster radio galaxies are also X-ray detections. The typical offset between the X-ray and point-like radio positions is 1″.5.

2.3. Optical

Optical spectra for Abell 2255 are available through the SDSS (Stoughton et al. 2002). These cover a wavelength range of 3800–9200Å with a resolving power of ~ 1900. They are collected using 640 3″ fibers per field, with successive 900-second exposures of a field being obtained until the cumulative median $(S/N)^2 > 15$ at $g^* = 20.2$ and $i^* = 19.9$ is achieved. For the region of Abell 2255, this typically amounted to 4500 seconds of exposure time. SDSS spectra were not available for objects #5 and #8. Their spectra, velocity, and classifications were obtained from Hill et al. (2003) and Miller & Owen (2003).

Figure 4 depicts the optical spectra of the X-ray selected cluster galaxies. None of these galaxies show the classical signs of harboring an AGN: two show the signatures of a starburst, one shows moderately strong Balmer absorption lines, and the rest have optical spectra characteristic of a passive galaxy.

3. Discussion

Searching for AGN using X-ray methods has been very productive. At energies above ~ 2 keV the X-ray sky is dominated by point sources and most of these are AGN (Mushotzky et al. 2000; Barger et al. 2002). This fact prompts us to use the superb angular resolution of *Chandra* to search for AGN emission in the eight X-ray detected objects in the central region of Abell 2255 associated with cluster galaxies. The eight objects cover a wide range in the L_X/L_{opt} plane with five of them (#1, #3, #4, #6, and #7) having X-ray to optical ratios (L_X/L_{opt}) much higher than those of field elliptical galaxies (see Figure 6). Objects #2, #5, and #8 have L_X/L_{opt} consistent with the brighter members of the Brown & Bregman (1998) elliptical galaxy sample. As Figure 7 shows, the five optically brightest X-ray sources seem to be drawn from the normal population of galaxies in Abell 2255, with $g^* - i^*$ colors similar to those of cluster elliptical and lenticulars.

The nature of these lower luminosity objects is not certain. We now know that there can exist ultra-luminous X-ray sources which are not AGN up to X-ray luminosities $L_X \approx 10^{41}$ ergs s^{-1} (Colbert & Ptak 2002), and it is possible that some of our sources can be associated with this type of object (e.g. source # 8). It is also possible that some of the X-ray emission can be due to hot gas in the galaxies as seen in the most luminous galaxies in Abell 1367 and the two massive central galaxies in the Coma cluster (Sun & Murray 2002; Vikhlinin et al. 2001). These latter galaxies have X-ray luminosities of 9.1×10^{40} and 7.6×10^{40} ergs s^{-1}, similar to our lowest luminosity objects. However, the uncertainties in the hardness ratios of our sources are not small enough to confirm that the emission is due to gas in elliptical

galaxies. Despite this, the combined X-ray, optical, and radio data are of sufficient quality to help constrain the nature of the eight detected objects.

Of the eight objects, we believe that two (#2, #6) are unambiguously associated with AGN and that source #8 may be an AGN. These galaxies have point-like *Chandra* emission with $L_X \approx 2.7 \times 10^{41}$ ergs s^{-1}, $L_X \approx 9.5 \times 10^{41}$ ergs s^{-1}, and $L_X \approx 3.8 \times 10^{41}$ ergs s^{-1}, respectively, plus hard X-ray spectra. Each galaxy is a powerful radio source, with #2 and #8 being head-tail sources and #6 a compact double. The optical spectra are pure absorption line dominated with no evidence for nuclear activity (see Figure 4).

Source #1 is rather enigmatic. Its *Chandra* image is point-like but at 7′ off axis the upper limit on source size is only 2″. It has a very high L_X/L_{opt} inconsistent with that of normal elliptical or starburst galaxies, and an optical spectrum indicative of a post-starburst galaxy (i.e., dominated by Balmer absorption lines; see Figure 4). Its X-ray spectrum is complex, requiring a thermal plus power law model, but the power law slope is relatively steep. There are indications from comparison of archival *ROSAT* data that the source was at least a factor of 3.5 times weaker when observed in 1993 and 1994 by the *ROSAT* PSPC and HRI. So the X-ray emission must be dominated by a small object, indicating that this source is either an AGN, an extremely luminous binary source (ULX), or perhaps a previously unrecognized ultra-luminous supernova.

Sources #3 and #7 appear to be starburst galaxies. Their X-ray emission from the *Chandra* observation is point-like and they have hard spectra. Optically, they are both fairly faint galaxies with strong, narrow emission lines representative of starbursts. Their radio fluxes are consistent with this description, and their X-ray to optical ratios are also consistent with starburst activity (Ranalli, Comastri, & Setti 2002). The relatively high ratio of hard to soft X-ray flux in source #3 is unusual for a starburst galaxy, although the lack of a significant number of counts limits this statement. Source #7 is fainter and has too few counts to even determine a flux ratio. In each case, the implied SFRs from the radio and X-ray emission are consistent to within about a factor of two. We note that other studies have also identified starburst galaxies dominated by very compact X-ray emission (e.g., NGC3256 Ward et al. 2000).

The X-ray emission of source #4 is not easily characterized. It appears to be slightly extended, with a Gaussian size of $\sim 3''$ ($6.2h_{50}^{-1}$ kpc) and a soft X-ray spectrum. While the galaxy is an interacting system, the X-ray emission is clearly associated with the southern elliptical galaxy. Its high L_X/L_{opt} is inconsistent with those of normal elliptical or starburst galaxies, and its optical spectrum is dominated by absorption lines. However, the extended nature of the emission indicates that the source is not dominated by a AGN. We conclude that this galaxy is similar to the X-ray emission observed from the cD galaxies in Coma

(Davis & Mushotzky 1993; Vikhlinin et al. 2001). It is interesting to note that without the *Chandra* evidence, this galaxy would almost certainly have been classified as an AGN. While many elliptical galaxies can have X-ray luminosities up to 10^{42} ergs s^{-1} produced by bremmstrahlung from hot gas (e.g., Davis & White 1996), their spectra are very soft and they are extended on scales of $\sim$10 kpc (Matsushita 2001). Observations made with instruments other than *Chandra* would fail to resolve the X-ray emission, which when coupled with its L_X/L_{opt} would result in classification as an AGN. It is therefore clear that classification based only on L_X/L_{opt} may be misleading.

Source #5 appears to be a "normal" elliptical galaxy. It is point-like in the *Chandra* image, but is relatively weak and consequently has a poorly determined X-ray spectrum. Optically, its spectrum, color, and magnitude are typical of cluster elliptical galaxies. Its X-ray to optical ratio is consistent with those of nearby non-AGN ellipticals (see Figure 6), suggesting that the X-ray emission arises from stars and diffuse hot gas in the galaxy.

As previously noted, the correspondence between the *Chandra* detections and the radio detections is excellent. It is instructive to consider this in light of the different classifications of the galaxies. On the basis of radio and optical properties, Miller & Owen (2003) classify eight of the 15 radio galaxies in the ACIS-I field as AGN. Five of these are detected in the present *Chandra* study, with the three non-detections being the three weakest radio sources out of the eight (their fluxes range from 0.36 mJy to 0.66 mJy; the weakest radio flux of the *Chandra* detected AGN is 1.43 mJy). The remaining seven radio sources consist of six star-forming galaxies and the post-starburst. Interestingly enough, the two star-forming galaxies detected by the *Chandra* observations correspond to the two optically-defined starburst galaxies, based on EW([OII])> 40Å (Dressler et al. 1999). Of the other four star-forming galaxies, two have stronger radio emission but are associated with larger galaxies whose spectra are more representative of a regular star formation history (although the optical spectrum of J171223+640829 has strong similarities to those of starburst galaxies).

There are several other *Chandra* papers which report the detection of point-like X-ray sources in clusters of galaxies: Abell 1367 (Sun & Murray 2002), Abell 2104 (Martini et al. 2002), Abell 1995 (Molnar et al. 2002), and RXJ003033.2+261819 and 3C295 (Cappi et al. 2001). Prior to *Chandra* , Lazzati et al. (1998) used *ROSAT* observations to identify point-like X-ray sources in Abell 194 and Abell 1367. In all of these papers most of the sources are less luminous than 3×10^{42} ergs s^{-1} (with the exception of one of the sources in Martini et al. (2002)) and show no evidence of optical nuclear activity. However, only Abell 2255 and Abell 1367 are close enough that the *Chandra* spatial resolution allows source classification. In Abell 1367, Sun and Murray report four new AGN and two new extended sources associated with hot gas, similar to the case in Abell 2255. Both the luminosity and

the classification of the sources in Abell 1367 are quite similar to that in Abell 2255.

We find that 5% of the luminous galaxies host low luminosity AGN, considerably above the values quoted from optical surveys in the literature (e.g., Dressler et al. 1999). We derive this by combining the statistics from Abell 2255, Abell 1367 and Abell 2104. To isolate the AGN the usual method is to select objects with high L_X/L_{opt} and flat X-ray spectra. But in the case of Abell 2255 it seems clear that at least one of the objects with high X-ray to optical ratio is a post-starburst galaxy and one is an elliptical galaxy with $\sim$10x the normal thermal X-ray flux.

The implications of the optical spectrum of source #1 warrant further discussion. Galaxies with post-starburst optical spectra are tied to the Butcher-Oemler effect (Butcher & Oemler 1978), as they are much more common in clusters at higher redshift than locally (e.g., Dressler et al. 1999). Their strong Balmer absorption implies a burst of star formation that has seemingly terminated within about the past Gyr. However, the sensitive radio observations of Smail et al. (1999) detected a large fraction of the post-starburst galaxies in the intermediate redshift cluster Cl 0939+4713. Galaxies with similar radio luminosities are typically powered by star formation, so the radio data might imply current star formation whose optical signatures are highly obscured by dust. In fact, the HST, optical and near-infrared imaging of Smail et al. seemed to confirm the presence of large amounts of patchy dust extinction. They thereby concluded that some galaxies with optical post-starburst spectra might be extreme examples of dust-obscured starbursts. The X-ray spectrum of the detected post-starburst galaxy in Abell 2255 is fit using a soft and a hard component, akin to the spectra of starbursts. Interestingly enough, it has the highest X-ray luminosity of all the detected sources in Abell 2255 (2×10^{42} ergs s^{-1}). In the local universe, the only star forming galaxies with luminosities greater than 10^{42} ergs s^{-1} are ultraluminous IR galaxies (Boller 1999; Condon et al. 1998) with IR luminosities above 10^{44} ergs s^{-1}. Thus, the magnitude of the X-ray emission (and the power law slope of the hard component) do not fit this picture. Similarly, the galaxy is detected in radio at a luminosity about an order of magnitude fainter than the post-starburst radio galaxies in Cl 0939+4713. This radio emission implies a star formation rate (SFR) about 50 times less than that derived from its X-ray emission (using the radio and X-ray SFR relationships found in Yun, Reddy, & Condon 2001; Ranalli, Comastri, & Setti 2002, respectively). Thus, while some residual star formation may be occuring, further explanation for the X-ray emission is required. It is possible that the high X-ray luminosity (arising mainly from the hard X-ray component) is caused by a large population of ULXs related to the recent starburst. However, since the X-ray flux has changed by a factor of at least 3.5 since the earlier *ROSAT* observations this is unlikely. A second possibility is that the starburst triggered an AGN in the galaxy. If it is an AGN, its X-ray spectral characteristics are most consistent with narrow-emission line

Seyfert galaxies (Leighly 1999) which often show both soft and hard components, or with BL Lac objects. There is one other similar source to our knowledge, NGC3862 (alias 3C 264, Sun & Murray 2002). This galaxy has a similar soft X-ray spectra and an optical spectrum lacking emission lines (but without strong Balmer absorption).

Of the eight galaxies that we have identified as cluster members, four of these are AGN (three ellipticals and the post-starburst galaxy; note that source #5 may also be an AGN) and none would be identified as such based on their optical spectrum. From this we deduce that in the central $16'$ of this cluster that the AGN fraction is $\sim 4\%$ (4/106). Adopting a canonical value of 1% based on the optically-derived AGN fraction, the probability of there being four AGN among the 106 cluster galaxies is only 1.8%. Despite the low total numbers, this is still significant at about 2.4σ level. As pointed out by Molnar et al. (2002) this fraction is a lower limit to the number of AGN in the cluster since we are not sensitive to AGN with high intrinsic column densities.

4. Conclusions

We find that, similar to the *Chandra* results for Abell 1367 and Abell 2104, there exists a population of point-like or small X-ray sources associated with the galaxies in Abell 2255. Three of these are clearly AGN, two are most probably starburst galaxies, one is an X-ray luminous elliptical dominated by hot gas, and two are of uncertain classification. The luminosity of the AGN are less than 3×10^{42} ergs s^{-1} and none of the host galaxies show optical evidence for activity. The most luminous object has a composite X-ray spectrum more reminiscent of a BL Lac or narrow line Seyfert galaxy and appears to be variable based on comparison of *ROSAT* and *Chandra* data. Interestingly, it is associated with a galaxy whose spectrum is that of a classical post-starburst. With several clusters now having similar properties we confirm the results from Martini et al, that the X-ray selected AGN fraction in clusters is much higher than optically selected AGN, similar to the results of the deep *Chandra* surveys (Barger et al. 2002), and these AGN tend to reside in red early-type galaxies. This is also consistent with the results of radio continuum studies.

REFERENCES

Arnaud, K. A., Astronomical Data Analysis Software and Systems V, eds. Jacoby G. and Barnes J., p17, ASP Conf. Series 101.

Barger, A.J., Cowie, L.L., Brandt, W.N., Capak, P., Garmire, G.P., Hornschemeier, A.E., Steffen, A.T., & Wehner, E.H. 2002, AJ, 124, 1839

Beers, T.C., Flynn, K., & Gebhardt, K. 1990, AJ, 100, 32

Bird, C.M. 1994, AJ, 107, 1637

Boller, T. 1999, Ap&SS, 266, 49

Brown, B.A., & Bregman, J.N. 1998, ApJ, 495, L75

Burns, J.O., Roettiger, K., Pinkney, J., Perley, R.A., Owen, F.N., & Voges, W. 1995, ApJ, 446, 583

Butcher, H. & Oemler, A. 1978, ApJ, 219, 18

Cappi, M., Mazzotta, P., Elvis, M., Burke, D.J., Comastri, A., Fiore, F., Forman, W., Fruscione, A., Green, P., Harris, D., Hooper, E.J., Jones, C., Kaastra, J.S., Kellogg, E., Murray, S., McNamara, B., Nicastro, F., Ponman, T.J., Schlegel, E.M., Siemiginowska, A., Tananbaum, H., Vikhlinin, A., Virani, S., & Wilkes, B. 2001, ApJ, 548, 624

Ciliegi, P., Bassani, L., & Caroli, E. 1995, ApJ, 439, 80

Colbert, E. & Ptak, A. 2002 ApJS, 143, 25

Condon, J.J., Yin, Q.F., Thuan, T.X., & Boller, T. 1998, AJ, 116, 2682

Cowie, L.L., Garmire, G.P., Bautz, M.W., Barger, A.J., Brandt, W.N., & Hornschemeier, A.E. 2002, ApJ, 566, L5

Davis, D.S., & Mushotzky, R.F. 1993, AJ, 105, 409

Davis, D.S., & White, R.E. III 1996, ApJ, 470, L35

Dickey & Lockman 1990, ARA&A, 28, 215

Dressler, A. & Gunn, J. E. 1983, ApJ, 270, 7

Dressler, A., Smail, I., Poggianti, B. M., Butcher, H., Couch, W. J., Ellis, R. S. & Oemler, A. 1999, ApJS, 122, 51

Edge, A.C., Steward, G.C., & Fabian, A.C. 1992, MNRAS, 258, 177

Elvis, M., Feigelson, E., Griffiths, R.E., Henry, J.P., & Tananbaum, H. 1980, Highlights of Astronomy, Volume 5 - International Astronomical Union, General Assembly, 17th, Montreal, Canada, August 14-24, 1979, Proceedings. (A81-19726 07-88) Dordrecht, D. Reidel Publishing Co., 1980, p. 653-656.

Feretti, L., Böhringer, H., Giovannini, G., & Neumann, D. 1997, A&A, 317, 432

Fukugita, M., Shimasaku, K., & Ichikawa, T. 1995, PASP, 107, 945

Garmire, G. P., Bautz, M. W., Ford, P. G., Nousek, J. A. & Ricker, G. R., Jr. 2003, Proc. SPIE, 4851, 28

Gómez, P.L., Loken, C., Roettiger, K., & Burns, J.O. 2002, ApJ, 569, 122

Hanisch, R.J. 1982, A&A, 111, 97

Hasinger, G. 2003, astro-ph/0302574

Hernquist, L. 1989, Nature, 340, 687

Hill, J.M., Miller, N.A., Oegerle, W.R., & Ganguly, R. 2003, in submission

Horner 2001 Ph.D. Thesis.

Jaffe, W.J., & Rudnick, L. 1979, ApJ, 233, 453

Jones, C., & Forman, W. 1984, ApJ, 276, 38

Kubo, H., Takahashi, T., Madejski, G., Tashiro, M., Makino, F., Inoue, S., & Takahara, F. 1998, ApJ, 504, 693

Lazzati, D., Campana, S., Rosati, P., Chincarini, G., & Giacconi, R. 1998, A&A, 331, 41

Ledlow, M.J., & Owen, F.N. 1995, AJ, 109, 853

Leighly, K.M. 1999, ApJS, 125, 317

Makishima, K., Kubota, A., Mizuno, T., Ohnishi, T., Tashiro, M., Aruga, Y., Asai, K., Dontani, T., Mitsuda, K., Ueda, Y., Uno, S., Yamoka, K., Ebisawa, K., Kohmura, Y. & Okada, K. 2000, ApJ, 535, 632

Martini, P., Kelson, D.D., Mulchaey, J.S., & Trager, S.C. 2002, ApJ, 567, 109

Matsushita, K. 2001, ApJ, 547, 693

Metevier, A. J., Romer, A. K. & Ulmer, M. P. 2000, AJ, 119, 1090

Miller, N.A., & Owen, F.N. 2002, AJ, 124, 2453

Miller, N.A., & Owen, F.N. 2003, AJ, 125, in press

Molnar, S.M., Hugher, J.P., Donahue, M., & Joy, M. 2002, ApJ, 573, L91

Mushotzky, R. F., Cowie, L. L., Barger, A. J. & Arnaud, K. A. 2000, Nature, 404, 459

Phillips, M.M., Jenkins, C.R., Dopita, M.A., Sadler, E.M., & Binette, L. 1986, AJ, 91, 1062
        (erratum 92, 503)

Ranalli, P., Comastri, A., & Setti, G. 2002, *astro-ph* 0202241

Sambruna, R. M., Eracleous, M. & Mushotzky, R. F. 1999 ApJ, 526, 60

Sadler, E.M., Jenkins, C.R., & Kotanyi, C.G. 1989, MNRAS, 240, 591

Smail, I., Morrison, G., Gray, M.E., Owen, F.N., Ivison, R.J., Kneib, J.-P., & Ellis, R.S.
        1999, ApJ, 525, 609

Stewart, G.C., Fabian, A.C., Jones, C., & Forman, W. 1984, ApJ, 285, 1

Stoughton et al. 2002, AJ, 123, 485 (SDSS)

Sun, M., Murray, S.S. 2002, ApJ, 577, 139

Vikhlinin, A., Markevitch, M., Forman, W., & Jones, C. 2001, ApJ, 555, L87

Ward, M.J., Zezas, A., Lira, P., Prestwich, A., Murray, S., Alonso-Herrero, A., & Ueno, S.
        2000, HEAD, 32, #18.05

Yee, H.K.C., Ellingson, E. 1993, ApJ, 411, 43

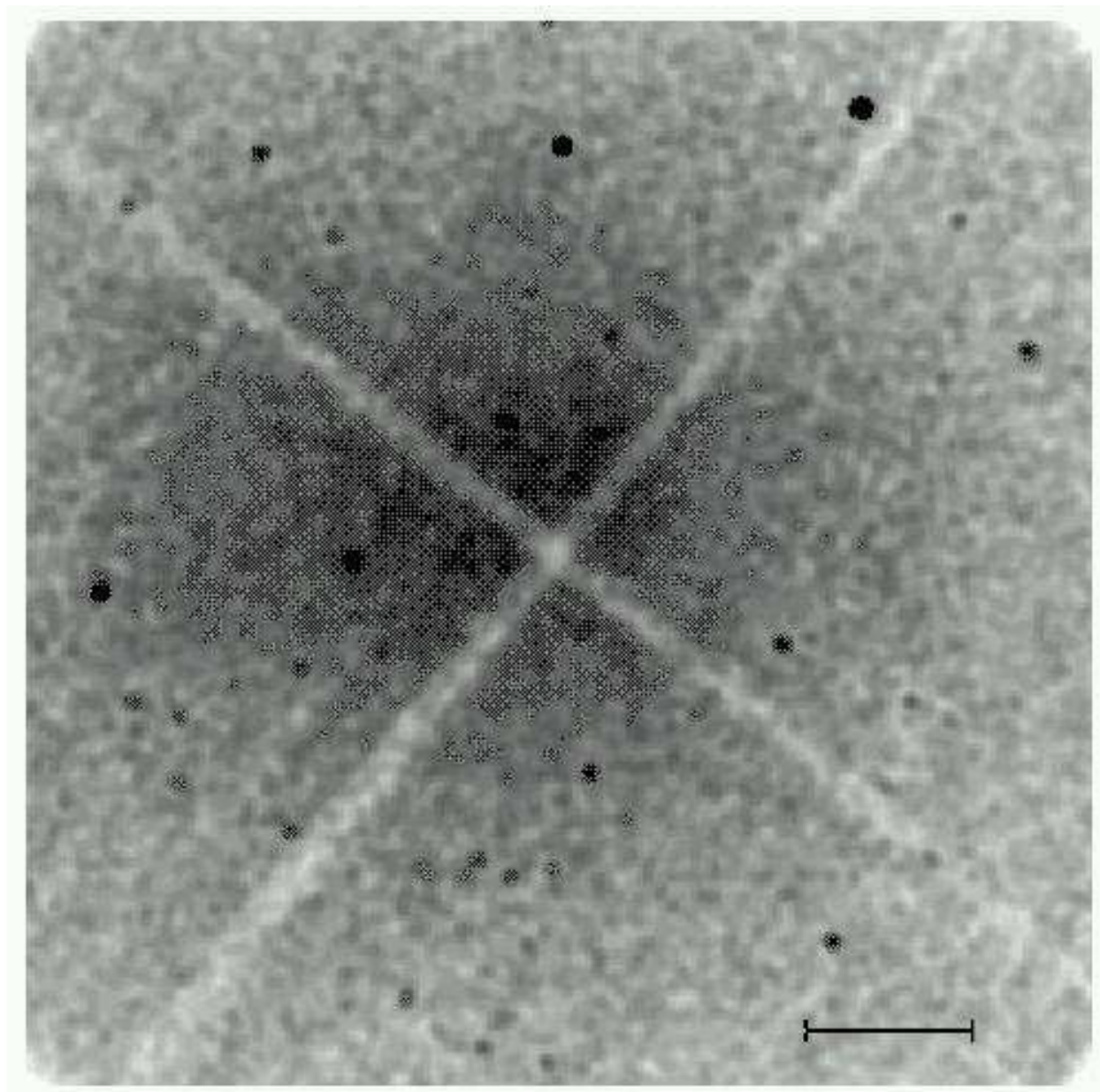Yun, M.S., Reddy, N.A., & Condon, J.J. 2001, ApJ, 554, 803

Fig. 1.— The exposure corrected and smoothed X-ray image of the Abell 2255 cluster in the 0.3 – 10 keV band. The bar in the lower right corner is $2'$ long and corresponds to 0.25 Mpc at the distance of the cluster. The image is oriented with north up and east to the left. The image is binned by a factor of 4 (1 pixel is $2''$) for display. The smoothing and constrast is choosen to emphasize point sources.
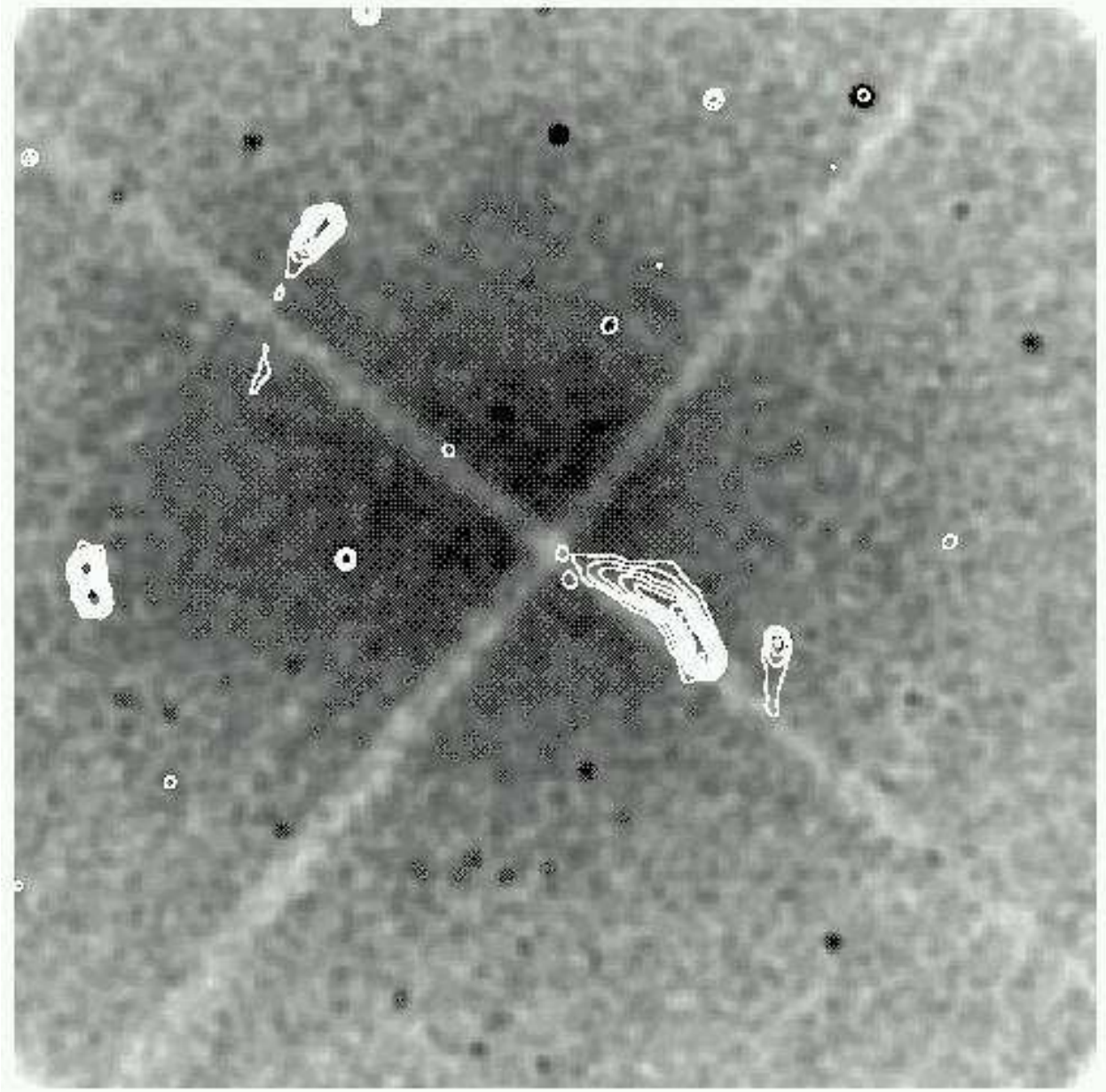
Fig. 2.— The smoothed X-ray image of Abell 2255 in the 0.3 to 10.0 keV band. The data for each of the chips is corrected for the exposure time for each chip. The radio contours are from Miller & Owen (2003).
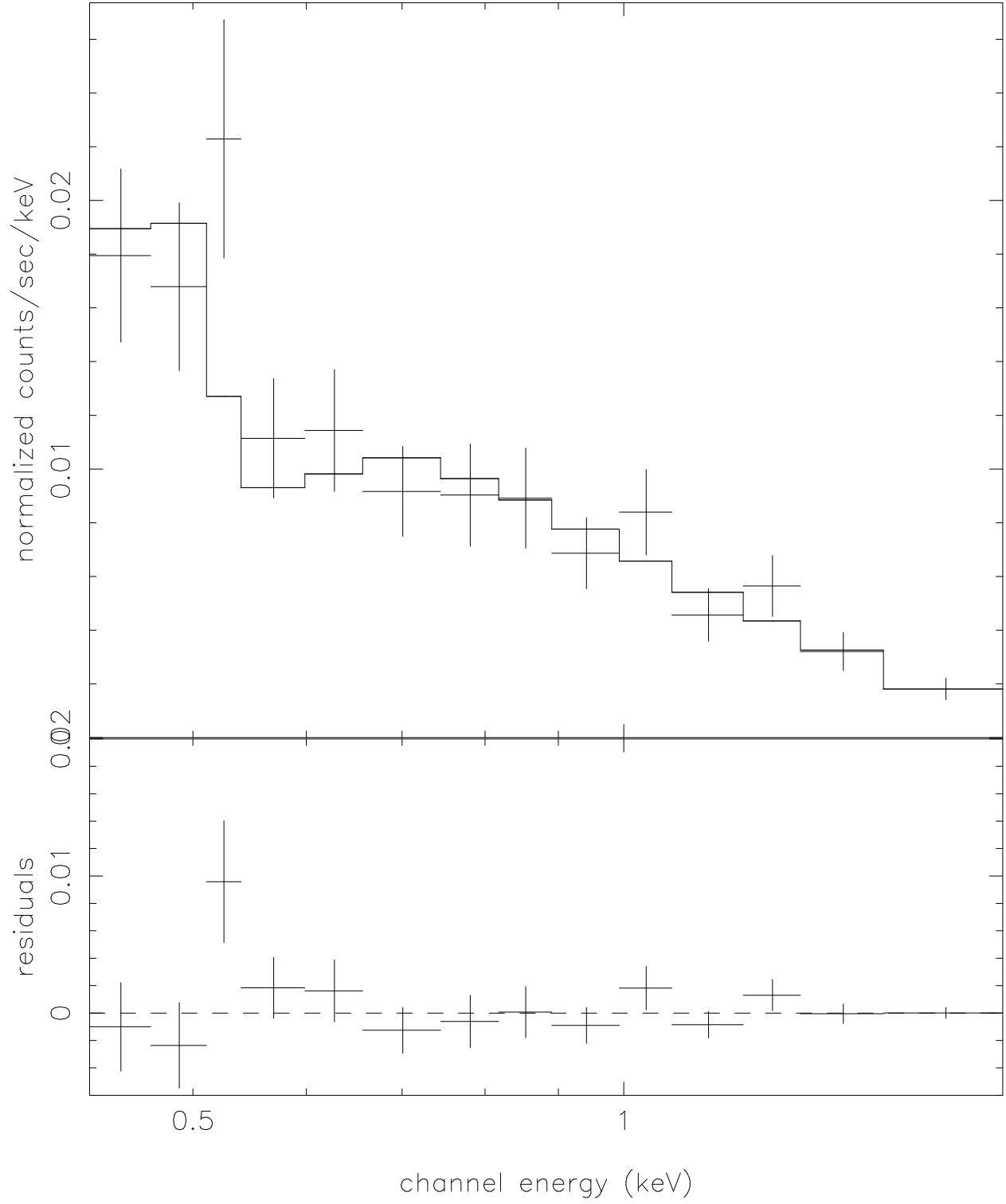
Fig. 3.— The extracted X-ray spectrum for source #1. The crosses are the data points and the solid line is the best fit power law plus a thermal plasma model.
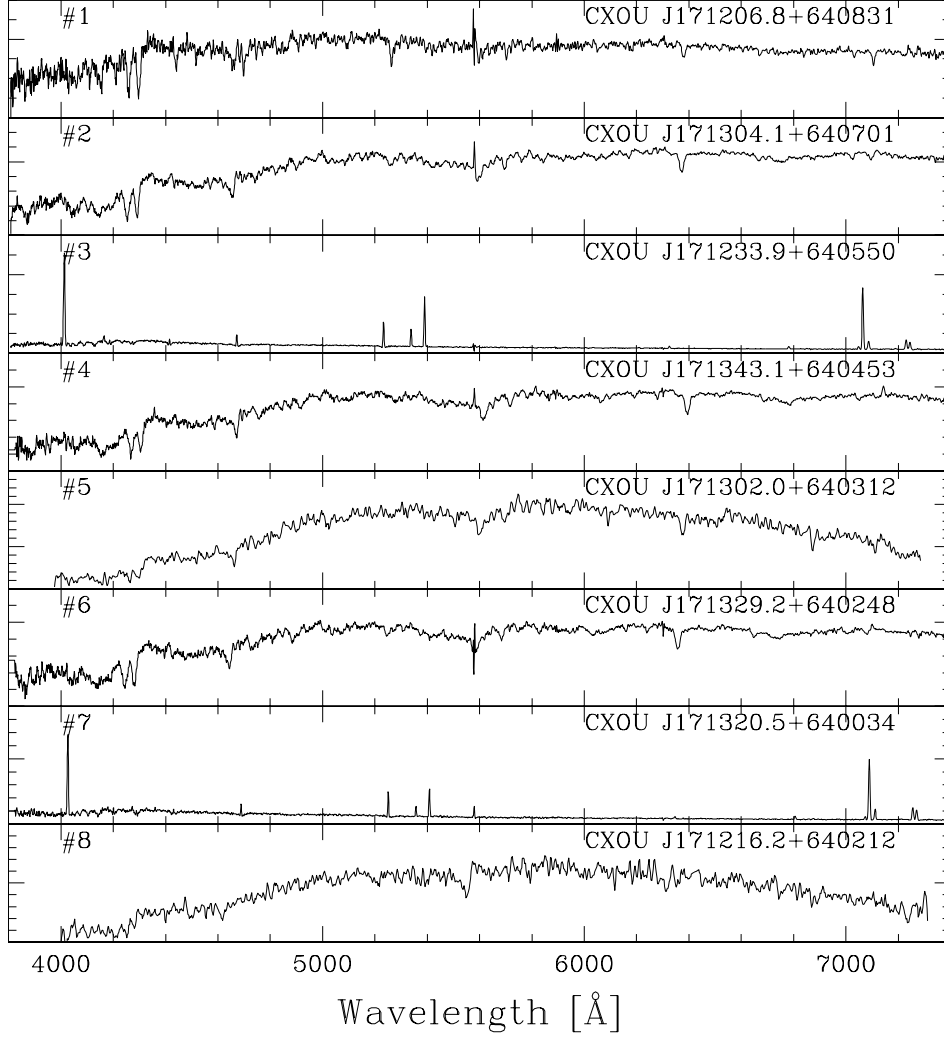
Fig. 4.— Optical spectra for the X-ray detected cluster galaxies. With the exception of #5 and #8, all are taken from the SDSS. Five of the galaxies (#2, #4, #5, #6, and #8) are easily distinguished as elliptical-like, lacking emission lines and with absorption features characteristic of older stellar populations. The spectrum of #1 is that of a post-starburst galaxy, with notable strong Balmer absorption and a relatively weak 4000Å break. The remaining galaxies, #3 and #7, have classic starburst spectra with strong narrow lines. The spectra have a resolution of $\sim$1900 and the vertical axis has been arbitrarily scaled for display.
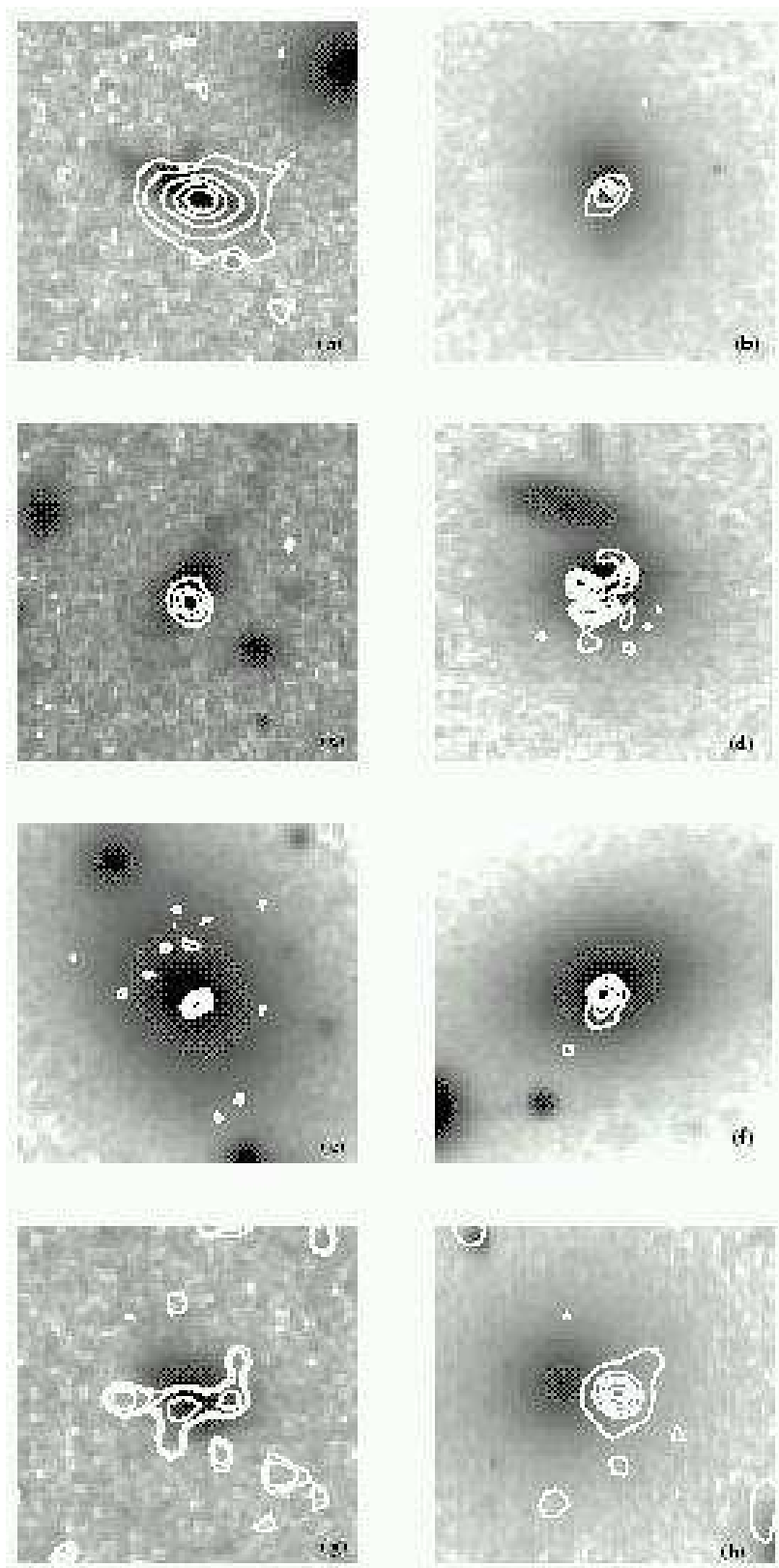
Fig. 5.— The X-ray contours from the exposure corrected and smoothed ACIS-I image in the 0.3 – 10.0 keV band overlaying the optical image from the KPNO 0.9 meter for the sources in table 1. The optical field covers 0.5′ on the sky. The image is oriented so that north is up and east is to the left. The apparent mismatch between the optical and X-ray is
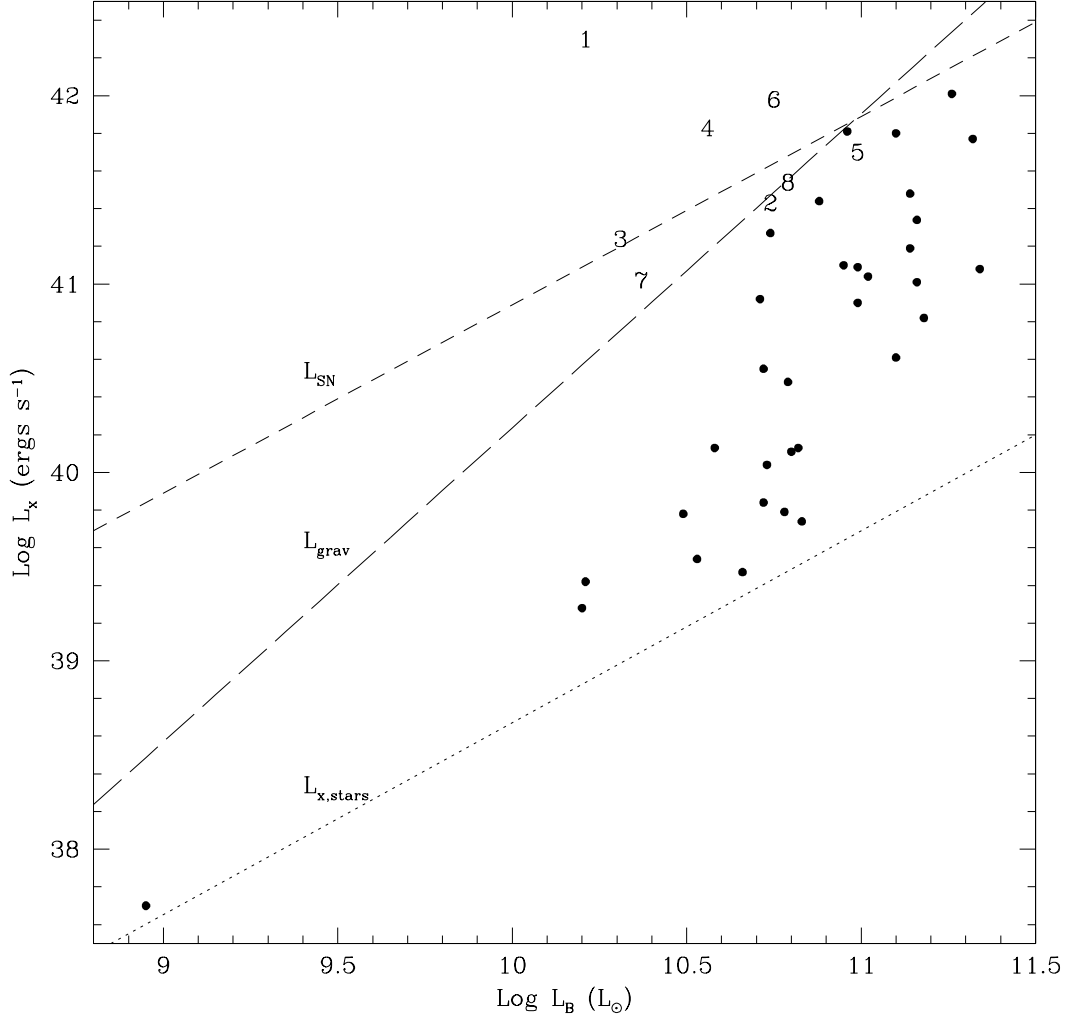
Fig. 6.— Correlation of X-ray luminosity with optical luminosity, for nearby normal elliptical galaxies (i.e., non-AGN). The solid points and expected relationships for X-ray luminosity from stellar emission (dotted line), gravitational energy release (long dashed line), and supernovae (dashed line) are taken from Brown & Bregman (1998). Points corresponding to the eight point X-ray point sources in Abell 2255 are indicated numerically (see Table 1 for the assignments). Their L_B values have been determined from their SDSS magnitudes using transformations from Fukugita, Shimasaku, & Ichikawa (1995).
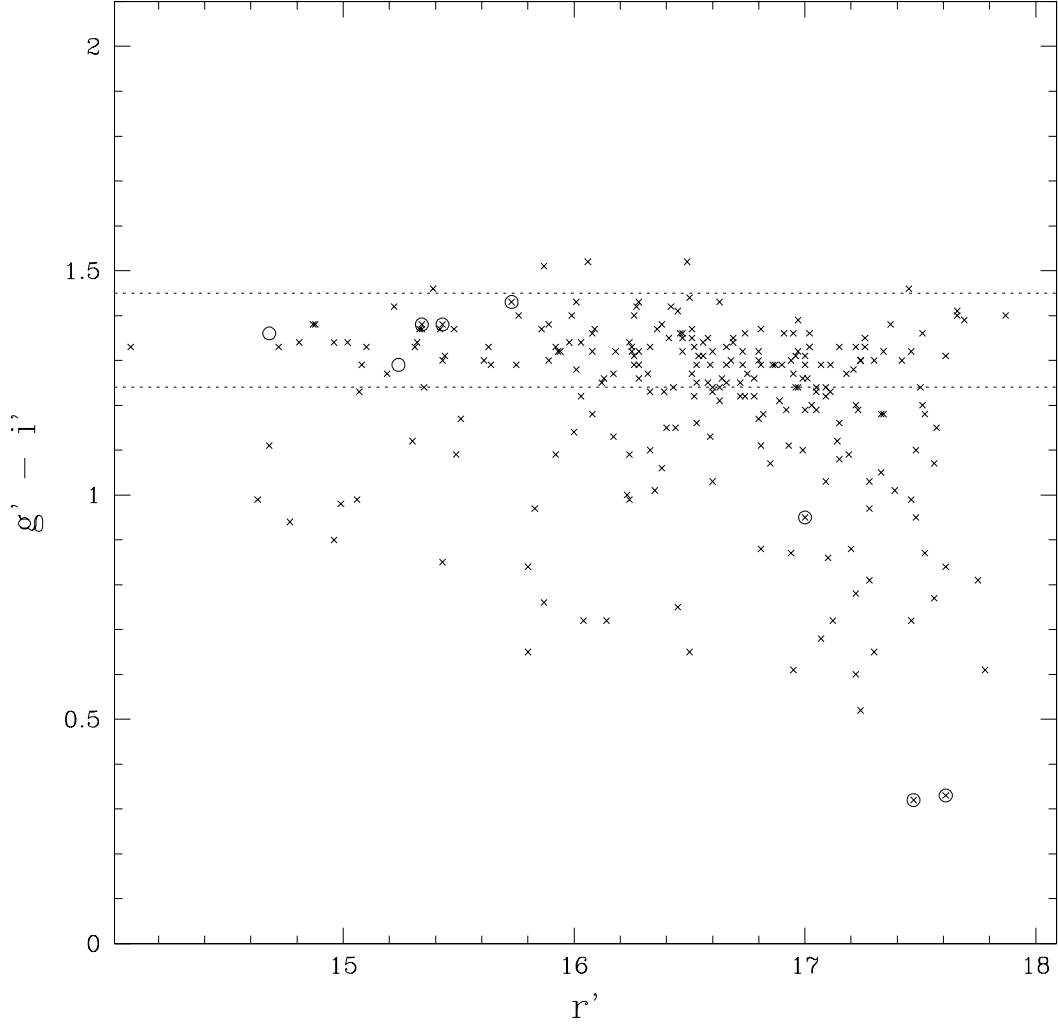
Fig. 7.— Color magnitude diagram for Abell 2255, based on SDSS data. Only galaxies with measured SDSS velocities are included. The dotted lines indicate the expected colors for cluster ellipticals and lenticulars, based on the transformations of Fukugita, Shimasaku, & Ichikawa (1995). The eight galaxies with associated X-ray point sources are indicated by circles; the fainter, blue galaxies are the starbursts (#3 and #7) and the next faintest galaxy is the post-starburst (#1).

Table 1.   Source Summary

ID	Name	Γ^a	L_x	$S_{1.4Ghz}$	r^*	g^*-r^*	cz (km/s)
1	CXOU J171206.8+640831	$2.98^{+0.86}_{-1.08}$	2.00×10^{42}	0.457	17.00	0.71	24671
2	CXOU J171304.1+640701	1.7^b	2.68×10^{41}	65.9	15.34	0.94	24243
3	CXOU J171233.9+640550	1.7^b	1.72×10^{41}	0.817	17.61	0.11	22838
4	CXOU J171343.1+640453	$\cdots$	6.69×10^{41}	2.766	15.73	1.00	25355
5	CXOU J171302.0+640312	$3.71^{+2.05}_{-1.28}$	5.04×10^{41}	1.430	14.68	0.97	24623
6	CXOU J171329.2+640248	$1.75^{+1.90}_{-0.78}$	9.48×10^{41}	248.3	15.43	0.90	23470
7	CXOU J171320.5+640034	1.7^b	$1.04\ \times10^{41}$	0.535	17.47	0.10	23950
8	CXOU J171215.6+640212	1.7^b	3.48×10^{41}	12.6	15.24	0.89	21416

[a]The fit for CXOU J171206.8+640831 includes a thermal plasma.

[b]Parameter is fixed.